Eidgenössische Technische Hochschule Zürich

Ecole polytechnique fédérale de Zurich
Politecnico federale di Zurigo
Swiss Federal Institute of Technology Zurich

Numerical Simulations of High Current Arc in Circuit Breakers

P. Huguenot, H. Kumar, V. Wheatley, R. Jeltsch, C. Schwab, M. Torrilhon

Research Report No. 2008-15
May 2008

Seminar für Angewandte Mathematik
Eidgenössische Technische Hochschule
CH-8092 Zürich
Switzerland

Numerical Simulations of High Current Arc in Circuit Breakers

P. Huguenot, H. Kumar, V. Wheatley, R. Jeltsch, C. Schwab, M. Torrilhon

Seminar für Angewandte Mathematik
Eidgenössische Technische Hochschule
CH-8092 Zürich
Switzerland

Research Report No. 2008-15 May 2008

Abstract

In a gas circuit breaker, a high temperature and pressure arc dissipates the tremendous amount of energy generated by the fault current, hence it protects the other parts of the circuit. Simultaneously this energy has to be transfered away from the contacts in order to protect the components of the circuit breaker. In this paper we present a model based on the three dimensional axis-symmetric equations of magnetohydrodynamics (MHD). This formulation allows us to study the behavior of the arc at very high currents. We generate numerical solutions in realistic, complex circuit breaker geometries, with real gas (SF_6) data using Runge-Kutta Discontinuous Galerkin (RKDG) methods. We study the various flow, thermal and electrical properties of the arc at high current.

Keywords: Make-Break Contacts, Arc phenomena, Magnetohydrodynamics.

1 Introduction

The main function of a circuit breaker is to switch off the electric current safely, in case of fault current. During the switching off of fault current many processes take place. When a fault current occurs, a mechanical force separates the contacts, and an arc starts to burn between the two contacts, due to the current flowing from the electrodes. This high-temperature arc dissipates large amount of energy. Simultaneously this energy has to be transfered away from the contacts in order to protect the components of the circuit breaker. In order to interrupt the current, the arc must be weakened and finally extinguished.

Plasma in the arc is consists of electrons, neutrons, ions and photons such that overall it is electrically neutral. Compared to an ordinary gas the plasmas are electrically conductive due to the presence of free charge particles. In fact, in many cases the conductivity of plasmas can be more than that of metals at the room temperature. Due to this property, plasma flows are very interesting to study because it involves both fluid dynamics properties and electric properties. Also fluid dynamics properties influence electric properties and vice-versa, i.e. the flow is both electrically and dynamically sensitive.

In order to study the arc behavior in the arc chamber of the circuit breaker, several theoretical approaches can be considered. Generally, these approaches do not exactly model all the phenomena in the arcing chamber and switching process. This is due to the complicated three dimensional geometry and involvement of various physical effects (like strong variation of conductivity) which make the computation of these model highly expansive.

In [3] Kovitya and Lowke derived a simple model for a plasma arc based on the Euler equations which are coupled with Ohm's law and Maxwell's equations for the magnetic field and are solved in a cylindrical coordinate system.

In [1] and [2] a more sophisticated 3D model has been derived. The effects of self induced magnetic fields and the external magnetic fields are studied. The mathematical model is based on the Navier-Stokes equation and Maxwell's equations which are solved simultaneously. Radiation terms are included. In [1] a two-dimensional, axis symmetric, free burning arc column at low current level is first modeled without the inclusion of self induced magnetic field. Then a three-dimensional air arc column at high-current levels with the self induced current are simulated. The numerical predictions are compared to analytical and experimental results. In [2] effects of the external magnetic fields and the gassing materials on a three-dimensional high current arc is simulated. More recently in [6] the behavior of the arc and the influence of external magnetic field is studied. The influence of nature of gas on the arc velocity is also studied. In [8] a reduced model for electric arcs based on energy equation coupled with eddy-current Maxwell equations was introduced. The existence and stability of this model is analyzed.

At very high currents (10kA-200kA), in the vicinity of the arc we expect the coupling between velocity and magnetic fields to be very strong due to high temperature produced by fault current. Due to this reason we consider a *strongly coupled* MHD model which is described in the Section 2 instead of a *weakly coupled* system of equations described in [1] and[6]. These equations model the flow of plasma under the influence of magnetic field with the evolution of the field itself. Main difficulty in computing these equations is presence of non-dimensional variable Lundquist number, $S_r = L_0 V_0 \mu_0 \sigma$, which at low conductivity leads to a very stiff system. To overcome this difficulty we use a *scaled conductivity* profile instead of the actual conductivity of the SF_6 gas. To solve this model we then use Runge-Kutta Discontinuous Galerkin methods which we will described in Section 3. In Section 4 we will describe the setting for our numerical simulations. The first simulation is designed to generate an arc with current 100kA, using the the artificial conductivity profile. In second simulation we study the effects of the external magnetic field and show that it is possible to generate a rotating arc at high currents. In last Section 5 we summarize our work.

2 The Mathematical Model

A true description of plasma motion must rely on kinetic equations for each plasma species. As this approach is too costly to simulate, a fluid description of the plasma is often used. This description is obtained by taking velocity moments of the kinetic equations describing a plasma under certain closure assumptions, and assumptions of large collision frequency. The Magnetohydrodynamics (MHD) are the equations give single fluid description of a plasma in which a single velocity and pressure describe both the electrons and ions. These equations in three dimensions then can be written in conservation form as given below,

- Mass conservation

$$\frac{\partial \rho}{\partial t} = -div\left(\rho \vec{v}\right) \tag{1}$$

- Momentum equation

$$\frac{\partial \left(\rho \vec{v}\right)}{\partial t} = -div\Bigg(\rho \vec{v}\vec{v}^t - \vec{B}\vec{B}^t + \left(p + \frac{1}{2}|\vec{B}|^2\right)\mathbf{I} - \frac{1}{S_v}\tau\Bigg) \tag{2}$$

- Magnetic field

$$\frac{\partial \vec{B}}{\partial t} = -curl\left(\vec{B} \times \vec{v} + \frac{1}{S_r} curl \vec{B}\right) \tag{3}$$

- Energy conservation

$$\frac{\partial E}{\partial t} = -div\Bigg((E+p)\,\vec{v} + \left(\frac{1}{2}|\vec{B}^2|\mathbf{I} - \vec{B}\vec{B}^t\right)\cdot\vec{v} - \frac{1}{S_v}\vec{v}\cdot\tau + \frac{1}{S_r}\left(\left(\vec{B}\cdot grad\right)\vec{B} - grad\left(\frac{1}{2}|\vec{B}^2|\right)\right) - \frac{1}{S_v P_r} gradT\Bigg) - S_d \quad (4)$$

To close the system we have equation of state,

$$E = \frac{p}{\gamma - 1} + \frac{1}{2}\left(\rho\vec{v}\cdot\vec{v} + |\vec{B}|^2\right) \quad (5)$$

The magnetic flux constraint,

$$div\vec{B} = 0, \quad (6)$$

has to be preserved over the time evolution.

In the equations above, ρ is density, $\vec{v}$ is velocity, $\vec{B}$ is magnetic field, p is pressure, T is temperature, and E is total energy per unit volume of the plasma. The physical properties of the plasma are the resistivity η, the thermal conductivity κ, the viscocity μ, and the ratio of the specific heats γ. They all are function of pressure and temperature for the real gas SF_6.

The non-dimensional parameters in the above equations are the Reynolds number, $R_e = \rho_0 V_0 L_0/\mu$, the Lundquist number, $S_r = \mu_0 V_0 L_0/\eta$ and Prandtl number, denoted by P_r, which is ratio of viscocity to thermal diffusitivity, i.e. $P_r = C_p\mu/\kappa$. The non-dimensionalization is carried out by using the circuit breaker length scale, L_0, Alfven speed $V_0 = B_0/\sqrt{\mu_0\rho_0}$, reference pressure P_0, reference temperature T_0 and ρ_0 is reference density. Also $\gamma = C_p/C_v$ is the ratio of specific heats and $\eta = 1/\sigma$, σ is the electrical conductivity. S_d is loss of energy due to radiation, given by Stefan Boltzman radiation law, $S_d = sT^4$, where $s = 5.6704 * 10^{-8}[J/sm^2K^4]$.

and the stress tensor τ is given by,

$$\tau = (\partial_j v_i + \partial_i v_j) - \frac{2}{3} div(\vec{v}\delta_{ij}), \quad (7)$$

which can be written in 3D as a 3×3-symmetric matrix

$$\tau = \begin{pmatrix} \tau_{11} & \tau_{12} & \tau_{13} \\ \tau_{21} & \tau_{22} & \tau_{23} \\ \tau_{31} & \tau_{32} & \tau_{33} \end{pmatrix}, \quad (8)$$

where $\tau_{11} = 2\frac{\partial v_1}{\partial_1} - \frac{2}{3}\nabla\cdot\vec{v}$, $\tau_{12} = \frac{\partial v_1}{\partial_2} + \frac{\partial v_2}{\partial_1}$, $\tau_{13} = \frac{\partial v_3}{\partial_1} + \frac{\partial v_1}{\partial_3}$, $\tau_{22} = 2\frac{\partial v_2}{\partial_2} - \frac{2}{3}\nabla\cdot\vec{v}$, $\tau_{23} = \frac{\partial v_3}{\partial_2} + \frac{\partial v_2}{\partial_3}$, $\tau_{33} = 2\frac{\partial v_3}{\partial_3} - \frac{2}{3}\nabla\cdot\vec{v}$, $\tau_{21} = \tau_{12}$, $\tau_{31} = \tau_{13}$, $\tau_{32} = \tau_{23}$.

These equations are then solved using appropriate boundary and initial condition for the simulation of a plasma arc, as described in Section 4, using the numerical algorithms explained in Section 3.

3 Algorithm for numerical solution of the PDE's

To perform numerical simulation of the equations (1)-(6) we use Nektar(see [7]) code. Nektar is developed at Brown University and uses a spectral-hp finite element algorithm, combined with a discontinuous Galerkin formulation for the advective and diffusive contributions, which provide the higher order approximation of the solution inside every cell but solution is allowed to be discontinuous across the edges of the cell (see [5]). The flow across the edges of the cells is determined by the flux across the boundary. These numerical fluxes are approximated using the approximated Riemann solvers. Limiters are used to make solution total variation diminishing if the shocks are present in the solution.

To perform three dimensional axis symmetric simulations we consider the equations (1)-(6) in cylindrical coordinates. This results in to equations containing partial derivatives with respect to radial (r), angular (θ) and axial (z) coordinates. Also velocity and magnetic fields are now given by $\vec{v} = (v_r, v_\theta, v_z)$ and $\vec{B} = (B_r, B_\theta, B_z)$. To enforce axis symmetry of the numerical solution we assume that derivatives with respect to θ-coordinate vanishes. So finally we have eight equations (for density, energy, three momentum and three magnetic fields), containing derivatives with respect to r and z coordinates only. We modify Nektar code to perform simulations of these equations. Real gas (SF_6) data is then implemented for computation of various physical parameters and equation of state.

4 Numerical Experiments

4.1 Generation of the arc

To generate the arc we consider the axisymmetric geometry given in Figure 1, with two arc roots C_1 and C_2, where the arc will be attached.

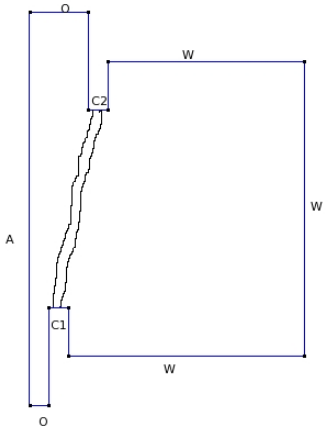

Figure 1: Geometry with rotation axis 'A', outflow boundaries 'O' and wall boundaries 'W'. The arc is burning between C_1 and C_2.

For these simulations we consider a reference length $L_0 = 10^{-3}m$, pressure $P_0 = 6 * 10^5$ Pa, temperature $T_0 = 300K$, density $\rho_0 = 35.13kg/m^3$. V_0 and B_0 are then calculated using relations given in Section 2. Also to remove the stability condition on time stepping we put $\mu_0 = 1.0$, which corresponds to replacing $\mu_0\sigma$ by σ. This is necessary due to stiffness of the system. We do realize that this can effect these results quantitatively, but we believe that qualitatively the results still hold. Study of effects of this scaling are contents of the future work.

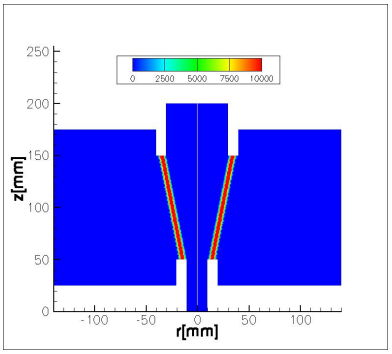

Figure 2: Initial artificial conductivity $\sigma[1/\Omega m]$

Initially, we assume that the arc has a constant thickness of 5mm. centered in the middle of arc root C_1 and C_2, so the shape of the initial arc is a cone. In this region we introduce a large artificial electric conductivity, see Figure 2. The artificial conductivity decays exponentially with time so that after dimensional time $t = 0.75ms$, the value of artificial conductivity is very low, compare to the physical conductivity.

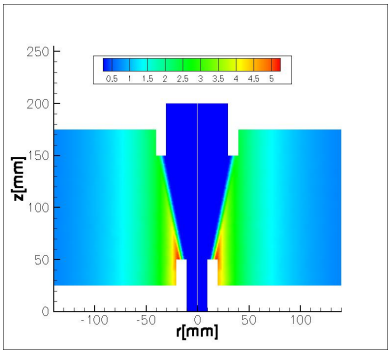

Figure 3: Initial magnetic field B_θ corresponding to constant current in the initial arc

Initial and boundary conditions in non-dimensional variables are given as follows,

- Initial conditions:

$$\begin{aligned} \rho &= 1 \\ \vec{v} &= 0 \\ P &= 1.0 \\ B_r &= 0 \\ B_z &= 0 \end{aligned} \tag{9}$$

Initial conditions for B_θ can be calculated by using the equations, 10) and 11. for the constant total current. Profile of B_θ from current is shown in Figure 3

$$\vec{B} = \frac{\mu_0 J r}{2} \qquad \text{Inside the arc} \tag{10}$$

$$\vec{B} = \frac{\mu_0 I}{2\pi r} \qquad \text{Outside the arc} \tag{11}$$

Where J is current density inside the arc, I is total current and r is the distance from the center of arc.

- Boundary conditions: outflow 'O'

$$\begin{aligned} \rho &= 1, \\ \vec{v} &= 0, \\ P = 1.0,\ \vec{B} &= 0, \end{aligned} \tag{12}$$

Wall boundary conditions are applied for velocity by inverting the normal component of velocity at the wall. Magnetic field conditions are applied by assuming no current condition. The following results were achieved using 6000 unstructured triangles, at time $T = 1.8ms$.

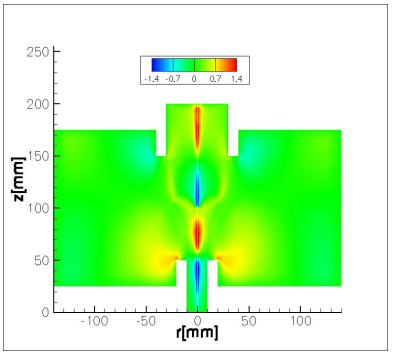

Figure 4: Non-dimensional axial velocity V_z

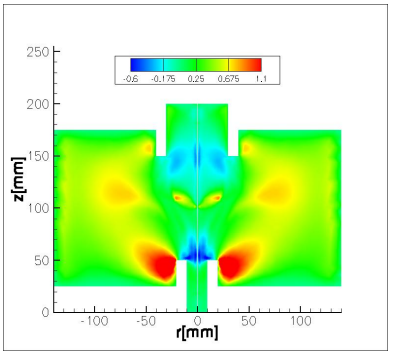

Figure 5: Non-dimensional radial velocity V_r

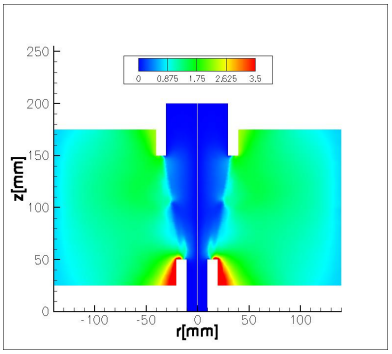

Figure 6: Non-dimensional angular magnetic field B_θ

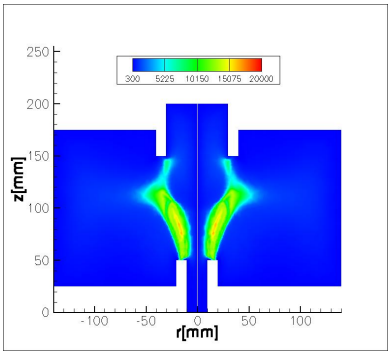

Figure 7: Temperature T in [K]

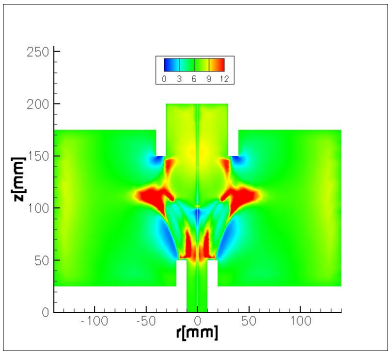

Figure 8: Pressure P in bar

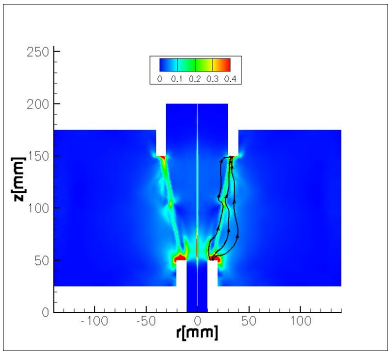

Figure 9: Non-dimensional current density J with current lines

4.2 Effects of external magnetic fields

In the rotating arc circuit breakers, the current that flows inside the arc also goes through a coil located below the cathode C_1. This coil generates a magnetic field in the whole region where the arc is burning, and brings the arc into rotation through Lorentz's force. In this Section we show the effect of a constant external magnetic field that is added to the previous solutions obtained in the Section 4.1. The external magnetic field was applied in the axial direction, i.e.

$$B_z = 0.05, \tag{13}$$

which corresponds to a dimensional magnetic field of $B_z = 0.043T$, using the formula in Section 2 for the scaling of the magnetic field. B_z is kept constant during time evolution. After a time $T = 3ms$ the following results were obtained:

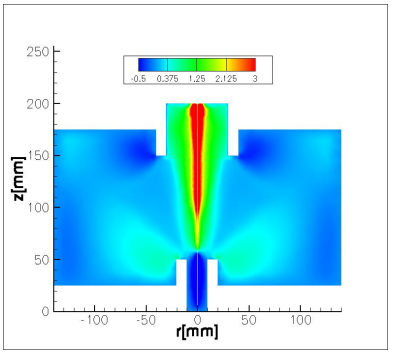

Figure 10: Non-dimensional axial velocity V_z

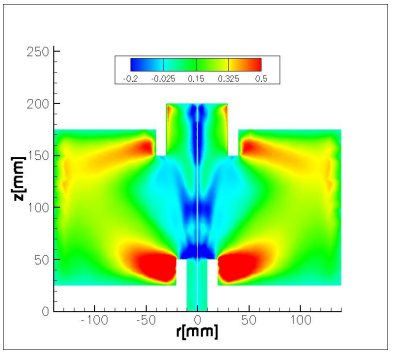

Figure 11: Non-dimensional radial velocity V_r

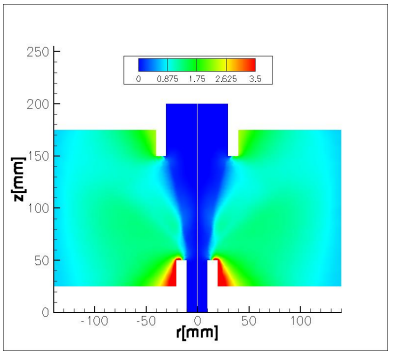

Figure 12: Non-dimensional angular magnetic field B_θ

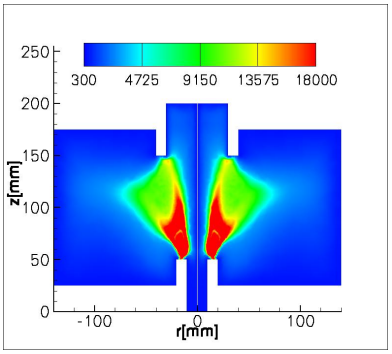

Figure 13: Temperature T in [K]

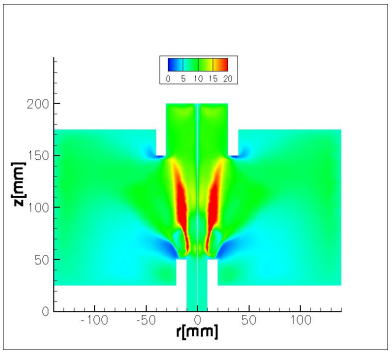

Figure 14: Pressure P in bars

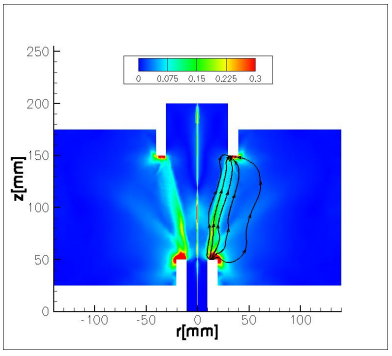

Figure 15: Non-dimensional current density J and current lines

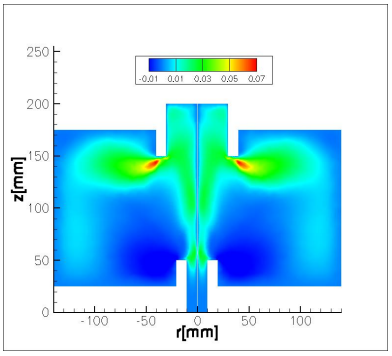

Figure 16: Non-dimensional angular velocity V_θ generated by axial magnetic field B_z

The effect of the external axial magnetic field is to generate an angular velocity that is shown in Figure 16. We can observe that the center and upper region of the arc is rotating in one direction, while the lower part near the cathode C_1 with the smaller radius rotates in the other direction but with smaller velocity. The pressure in the arc and in its vicinity is also increased.

The maximal nondimensional angular velocity is $V_\theta = 0.07$ (see Figure 16). Using the scaling equation $V_0 = \sqrt{P_0/\rho_0}$ (see Section 2), this corresponds to a velocity of $V_\theta = 9.15m/s$. Considering an arc radius of 10mm, we find a rotation frequency of 147 Hz.

5 Conclusion

We showed that high current arc simulation can be achieved using the equations of Magnetohydrodynamics. In the axisymmetric case, the effect of an external axial magnetic field is to generates an angular motion that can be used to increase the pressure build up around the arc.

References

[1] Lei Z. Schlitz, Suresh V. Garimella, S. H. Chan,*Gas Dynamics and electromagnetic processes in high-current arc Plasmas. Part I Model Formulation and steady state solutions* , Journal of Applied Physics, 85(5),1999, pp 2540-2546

[2] Lei Z. Schlitz, Suresh V. Garimella, S. H. Chan,*Gas Dynamics and electromagnetic processes in high-current arc Plasmas. Part II Effects of external magnetic fields and gassing materials* , Journal of Applied Physics, 85(5),1999, pp 2547-2555

[3] P. Kovitya, J. J. Lowke ,*Two-Dimensional analysis of free burning arcs in argon* , J. Phys. D: Appl. Phys., 18,1985, pp 53-70.

[4] L. Niemeyer, W. Widl *Rotating Arcs in SF_6-Circuit-Breakers*, ABB Research Center 5405 Baden.

[5] George Karniadakis and Spencer Sherwin, *Spectral/hp Element Methods for Computational Fluid Dynamics* , Oxford University Press (2005).

[6] B Swierczynski, J J Gonzalez, P Teulet, P Freton, A Gleizes *Advances in low-voltage circuit breaker modelling*, J. Phys. D: Appl. Phys., 37,2004, pp 595-609.

[7] Guang Lin and George Em Karniadakis, *A discontinuous Galerkin Method for Two-Temperature Plasmas*, Brown University (2004)

[8] M. Torrilhon *Stability of reduced electric arc models*, Proc. ICIAM 2007.